CHAPTER

6

Thermal Studies on Some Copper(I) Complexes of Dithiocarbamates Derived from Primary Amines

6.1. Introduction

The thermal properties of metal dithiocarbamate complexes have been extensively investigated as one of the most interesting topics in the field of coordination chemistry. In metal dithiocarbamates, thermal analysis data have been utilised to (a) investigate the limit of horizontal stretch between which the complex retains the assigned formula (b) study the mode of thermal decomposition of metal complexes (c) determine the optimum temperature range for the resulting products to attain constant weight, thereby affording standardisations of the conditions for the gravimetric evaluation of metal ions (d) evaluate the activation energy and other kinetic parameters and assign the solid state reaction mechanism for each stage of thermal decomposition and so on. The earliest work on the thermoanalytical investigation of metal dithiocarbamates was in 1905 by Delepine who found that Ni(II) and Cu(II) di-isopropyl dithiocarbamates sublime in vacuum almost without decomposition.[1,2] D' Ascenzo and Wendlandt[3] found that the Co(II), Ni(II), Cu(II), Zn(II), Cd(II), Ag(I) and Hg(II) diethyldithiocrbamates were volatile in an inert atmosphere. The volatility of some of the metal

dithiocarbamates have been used to develop gas chromatographic methods for separating metals[4-7] and analysis of metals by atomic absorption spectroscopy.[8] Reports on thermal behaviour of a large number of metal dialkyldithiocarbamates indicate that formation of metal thiocyanate intermediate is the essential step in the decomposition of the majority of dithiocarbamate complexes, the final product being metal sulphide or oxide.[9] In certain copper and platinum dithiocarbamates the composition of the end product does not correspond to either pure metal or sulphide; this may be attributed to the formation of non stoichiometric metal sulphides at high temperature.[10,11]

Thermal studies on metal complexes of primary amine derived dithiocarbamates are not so numerous.[12-21] Thermal behaviour of $M(S_2CNH_2)_2$ complexes were reported by Bernard and Borel.[22] These complexes were found to decompose with the evolution of H_2S or CS_2. According to Venkappayya and Brown[23] primary amine-derived dithiocarbamates like N-α-methyl benzyl dithiocarbamates of Cr(III), Co(II), Ni(II), Zn(II) and Cd(II) undergo thermal decomposition with the loss of H_2S. The presence of hydrogen atom on nitrogen seems to facilitate loss of H_2S and the formation of isothiocyanate as an intermediate during the thermal decomposition. In every case, sulphide or its oxidised product, was identified as the product of decomposition indicating breaking of carbon-sulphur bond. From a survey of the literature it seems that very little work has been reported on the kinetics and reaction mechanism of thermal decomposition of dithiocarbamates.[24,25] In the present study on the thermal behaviour of Cu(I) complexes of various N-monosubstituted dithiocarbamates, the mode of their thermal decomposition and relation between structure and thermal stability are discussed. Kinetic parameters have been calculated and reaction mechanisms for all the major decomposition steps proposed.

6.2. Experimental

Preparation of the dithiocarbamate ligands and the corresponding Cu(I) complexes and the thermoanalytical methods employed are already discussed in Chapters **2, 3** and **4.** In the present investigation seventeen complexes representing both oligomers and polymers derived from a variety of N-monosubstituted dithiocarbamates are studied. The complexes studied for thermal behaviour are the following.

(i) $[Cu(BuHNCS_2)]_2$, (ii) $[Cu(BzHNCS_2]_4$, (iii) $[Cu(BuHNCS_2)]_n$,
(iv) $[Cu(BzHNCS_2)]_n$, (v) $[Cu(EtHNCS_2)]_n$, (vi) $[Cu(PAHNCS_2)]_2$,
(vii) $[Cu(CmHNCS_2)]_n$ (viii) $[Cu(PhHNCS_2)]_4$, (ix) $[Cu(mCHNCS_2)]_4$,
(x) $[Cu(mTHNCS_2)]_4$, (xi) $[Cu(oAHNCS_2)]_2$, (xii) $[Cu(oTHNCS_2)]_2$,
(xiii) $[Cu(PhHNCS_2)]_n$ (xiv) $[Cu(mCHNCS_2)]_n$ (xv) $[Cu(pCHNCS_2)]_n$,
(xvi) $[Cu(pTHNCS_2)]_n$ and (xvii)$[Cu(pAHNCS_2)]_n$.

All the complexes were subjected to TG and DTG analysis up to 800° C in nitrogen atmosphere.

Mathematical treatment of data

Deduction of the mechanism of thermal decomposition process from non-isothermal TG curves has been discussed by Sestak and Berggren.[27] The procedure is based on the assumption that the non-isothermal reactions proceeds isothermally at an infinitesimal time interval, so that the rate, $\frac{d\alpha}{dt}$, can be expressed by an Arrhenius type equation

$$\frac{d\alpha}{dt} = A e^{-E/RT} f(\alpha) \qquad (6.1)$$

where A is the pre-exponential factor and $f(\alpha)$ depends on the mechanism of the process involved. For a linear heating rate, ϕ, $dT/dt = \phi$ and substitution into Eqn. (6.1) gives

$$\frac{d\alpha}{f(\alpha)} = \frac{A}{\phi} e^{-E/RT} dT \qquad (6.2)$$

On integration, taking initial temperature as zero (this assumption is correct as no reaction occurs between T = 0 and T = T_i)

$$\int_0^{\alpha} \frac{d\alpha}{f(\alpha)} = g(\alpha) = \frac{A}{\phi} \int_0^{T} e^{-E/RT}\, dT \qquad (6.3)$$

where g(α) is the integrated form of f(α). In the usual non-mechanistic kinetic equations like, for example, Coats and Redfern equation, it is assumed that $f(\alpha) = (1-\alpha)^{1-n}$ where n is the order parameter. In contrast, mechanistic kinetic studies are based on the assumption that the form of f(α) depends on the reaction mechanism. A series of f(α) forms are proposed and the integrated form $\int_0^{\alpha} \frac{d\alpha}{f(\alpha)} = g(\alpha)$ for nine probable reaction mechanisms, listed by Satava, are given in Table 6.1.

Table 6.1. Commonly used g (α) form for solid state reactions

Equation No.	Form of g(α)	Rate controlling process
1	$-\ln(1-\alpha)$	Random nucleation one nucleus on each particle (Mampel equation).
2	$1-(1-\alpha)^{1/2}$	Phase boundary reaction, cylindrical symmetry
3	$1-(1-\alpha)^{1/3}$	Phase boundary reaction, spherical symmetry
4	$(1-\alpha)\ln(1-\alpha)+\alpha$	Two dimensional diffusion, cylindrical symmetry
5	$(1-\frac{2}{3}\alpha)-(1-\alpha)^{2/3}$	Three dimensional diffusion, spherical symmetry (Ginstling-Brownshtein equation)
6	$-\ln(1-\alpha)^{1/2}$	Random nucleation (Avrami equation I)
7	$-\ln(1-\alpha)^{1/3}$	Random nucleation (Avrami equation II)
8	$[1-(1-\alpha)^{1/3}]^2$	Three dimensional diffusion, spherical symmetry (Jander equation)
9	α^2	One dimensional diffusion.

For evaluating kinetic parameters from the mechanistic equations, the right-hand side of Eqn. (6.3), temperature integral which is an incomplete gamma function was used in the form given by Coats and Redfern.[28]

$$\frac{\ln g(\alpha)}{T^2} = \ln \left[\frac{AR}{\phi E} \frac{(1-2RT)}{E} \right] - \frac{E}{RT} \qquad (6.4)$$

Linear plots of the nine forms of $\frac{g(\alpha)}{T^2}$ versus $\frac{1}{T}$ were drawn by the least square method and the corresponding correlation coefficients were also evaluated. E and A were calculated in each case from the slope and intercept respectively. The mechanism is obtained from the form of $g(\alpha)$ which gives the best representation of the experimental data. The entropy of activation was calculated using the equation $A = \frac{KT_s}{h} e^{-\Delta S/R}$, k is Boltzman constant, h = Planks constant and T_s = DTG peak temperature.

6.3. Results and discussion

All the complexes under the present thermal study have been characterised by elemental analysis, molecular mass determination, infrared and electronic spectra as well as ESR and magnetic susceptibility measurements (Chapters **3** and **4**). Information on the structure and stereochemistry of these complexes was also provided by the study of the effect of the N-substituents of Dtc on the polymerising tendency of the corresponding Cu(I) complex in aqueous medium during their preparation and also by the study of the reactivity characteristics of the complex towards electrophilic substitution reaction like benzoylation (Chapter **4**). Thermal analysis of these representative 17 complexes was attempted to confirm the conclusions already arrived at regarding their composition and structural features and also to examine, to some extent, the relation between thermal

stability and structure. Phenomenological, kinetic and mechanistic aspects of thermal decomposition of all the complexes are discussed.

6.3.1 Phenomenological aspects

As mentioned earlier both oligomeric (dimeric and tetrameric) and polymeric copper(I) complexes of mono alkyl/aryl substituted dithiocarbamates were isolated by adopting appropriative techniques. Since for the compounds with same composition the nature of decomposition is seen dependent on the degree of aggregation/polymerisation, their phenomenological aspects are discussed separately.

(a) N-alkyl dithiocarbamato copper(I)

(i) Oligomers

The TG and DTG curves of the two complexes belonging to this category, $[Cu(BuHNCS_2)]$ and $[Cu(BzHNCS_2)]_4$ are presented in Figures 6.1 and 6.2.

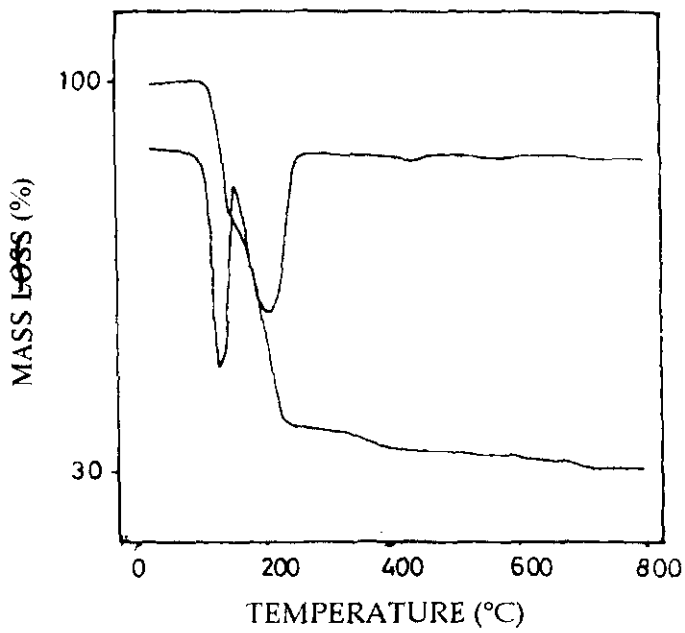

Figure 6.1. TG and DTG curves of $[Cu(BuHNCS_2)]_2$ in nitrogen atmosphere

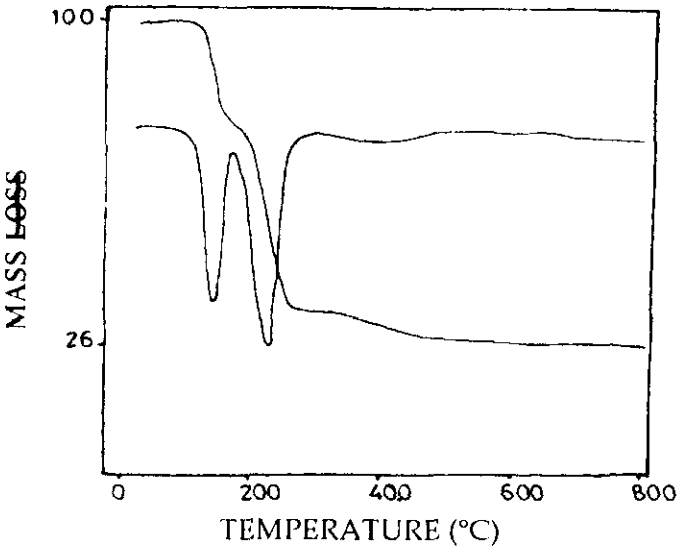

Figure 6.2. TG and DTG curves of [Cu (BZHNCS$_2$)]$_4$ in nitrogen atmosphere

The temperature ranges and percentage mass losses during the decompositions as well as the temperature corresponding to the maximum rate of decomposition, DTG_{max} and the theoretical percentage mass losses are given in Table 6.2. Both the complexes show three stage weight loss in their TG and DTG curves. The decomposition begins at 105 and 111°C, respectively, in these complexes.

Table 6.2. Thermal decomposition data

Compound	Stage	Decomp. temp. range (°C)	DTG_{max} (°C)	Mass loss (%) found (calcd.)	Evolved moiety*
[Cu (BuHNCS$_2$)]$_2$ (A)	I	111-167	131	27.3 (27.2)	-RNCS
	II	167-278	206	36.2 (35.2)	-(RNCS + H_2S)
	III	278-700	373	7.0 (7.3)	-S
	R**			29.5 (30.0)	2 Cu**
[Cu (BzHNCS$_2$)]$_4$ (B)	I	106-172	139	22.7 (23.3)	-RNC
	II	172-283	228	433 (438)	-(RNCS +H_2S+S)
	2	283-700	427	7.8 (6.5)	-S
	R**			26.2 (25.9)	2 Cu**

*Evolved moiety corresponding to each dimeric unit
**Residue

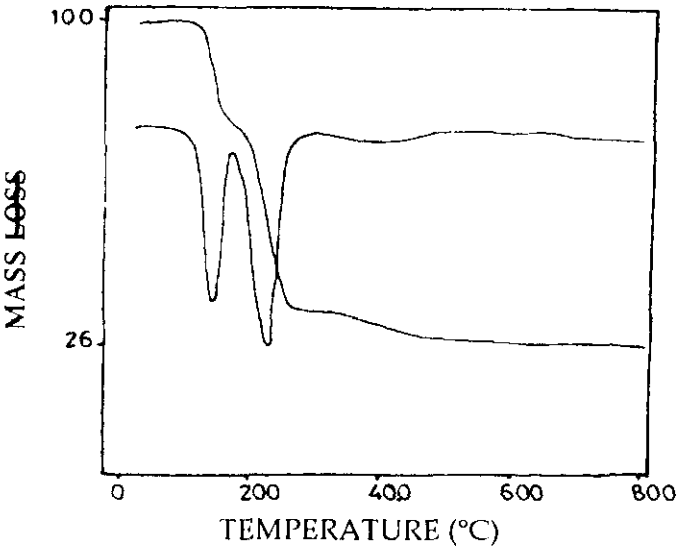

Figure 6.2. TG and DTG curves of [Cu (BZHNCS$_2$)]$_4$ in nitrogen atmosphere

The temperature ranges and percentage mass losses during the decompositions as well as the temperature corresponding to the maximum rate of decomposition, DTG_{max} and the theoretical percentage mass losses are given in Table 6.2. Both the complexes show three stage weight loss in their TG and DTG curves. The decomposition begins at 105 and 111°C, respectively, in these complexes.

Table 6.2. Thermal decomposition data

Compound	Stage	Decomp. temp. range (°C)	DTG_{max} (°C)	Mass loss (%) found (calcd.)	Evolved moiety*
[Cu (BuHNCS$_2$)]$_2$ (A)	I	111-167	131	27.3 (27.2)	-RNCS
	II	167-278	206	36.2 (35.2)	-(RNCS + H_2S)
	III	278-700	373	7.0 (7.3)	-S
	R**			29.5 (30.0)	2 Cu**
[Cu (BzHNCS$_2$)]$_4$ (B)	I	106-172	139	22.7 (23.3)	-RNC
	II	172-283	228	433 (438)	-(RNCS +H_2S+S)
	2	283-700	427	7.8 (6.5)	-S
	R**			26.2 (25.9)	2 Cu**

*Evolved moiety corresponding to each dimeric unit
**Residue

The decomposition begins at 149, 165 and 147°C, respectively in these complexes. The complexes C, A and B undergo one-stage, two-stage and three stage decomposition respectively. The final product in all the cases was found to be Cu_2S_2. Copper and sulphur content in the residues were confirmed by elemental analysis. Copper is not seen existing in the cupric state which was also confirmed by the absence of any signal in the EPR spectrum of these residues. The TG and DTG curves of the three complexes are presented in Figures 6.3-6.5.

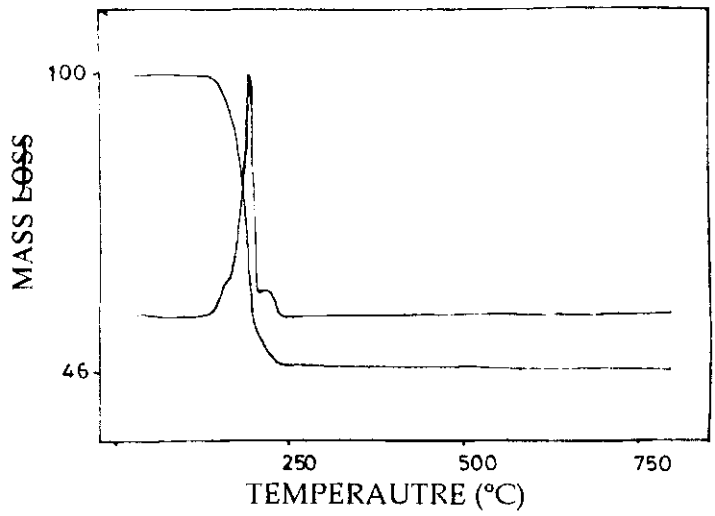

Figure 6.3. ***TG and DTG curves of $[Cu(BuHNCS_2)]_n$ in nitrogen atmosphere***

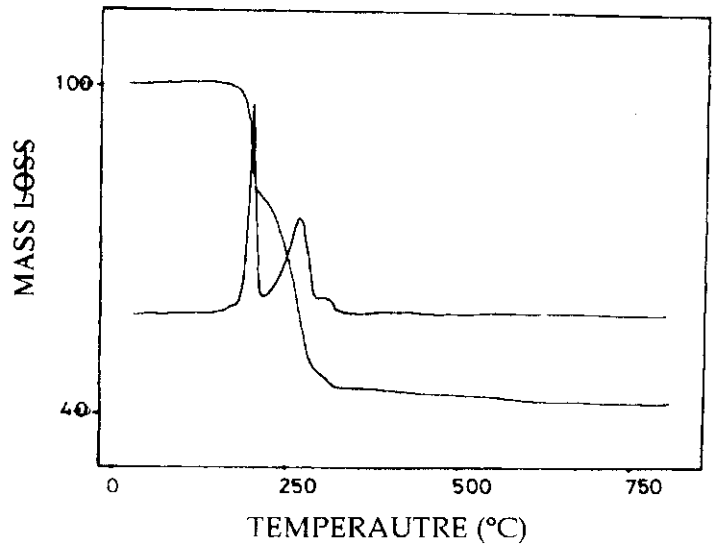

Figure 6.4. ***TG and DTG curves of $[Cu(BzHNCS_2)]_n$ in nitrogen atmosphere***

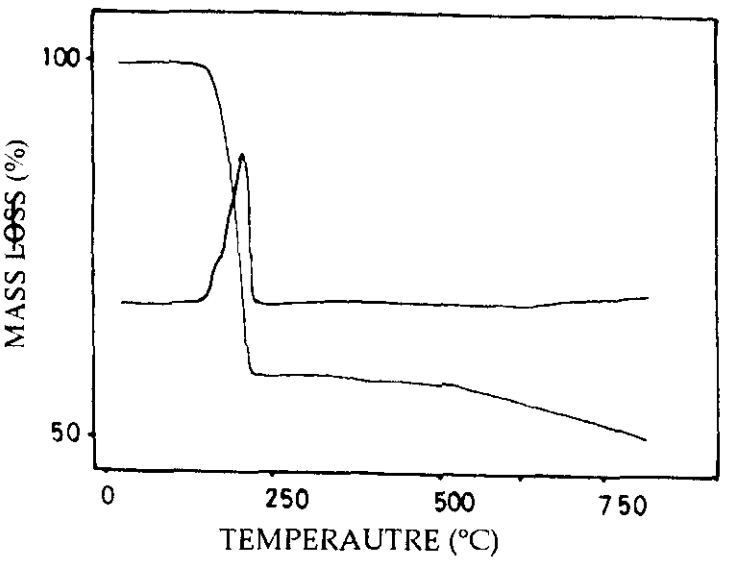

Figure 6.5. TG and DTG curves of $[Cu(EtHNCS_2)]_n$ in nitrogen atmosphere

(b) N-aryl dithiocarbamato copper(I)

(i) Oligomers

The phenomenological data of thermal decomposition of the tetrameric complexes $[Cu(PhHNCS_2)]_4$, $[Cu(mCHNCS_2)]_4$ and $[Cu(mTHNCS_2)]_4$ and dimeric complexes $[Cu(oAHNCS_4)]_2$ and $[Cu(oTHNCS_2)]_2$ are presented in Table 6.4. On the basis of stoichiometric calculations, the tentative assignment of the evolved moieties during each stage of decomposition are also presented in the table. All the complexes except A starts decomposing at about 100°C. The initial decomposition temperature for A is about 122°C. D decomposes in a single stage. All the other complexes decompose in two stages, the mass loss being almost complete below 500°C. On the basis of stoichiometric calculations the final residues per dimeric unit are (A) 2Cu, (B) Cu_2S_2, (C) Cu_2S, (D) 2Cu and (E) Cu_2S_2. It was confirmed by qualitative analysis that the residue of A and D contained copper only while those of B, C and E contained both copper and sulphur. The TG and DTG curves of all the five complexes are given in Figures 6.6-6.10.

Table 6.4. Thermal decomposition data

Compound	Stage	Decomp. temp. range (°C)	DTG_{max} (°C)	Mass loss (%) found (calcd.)	Evolved moiety*
$[Cu(PhHNCS_2)]_4$ (A)	I	122-311	189	51.8 (53.7)	-(2 RNC + H_2S)
	II	311-639	500	20.6 (20.7)	-3S
	R**			25.7 (27.4)	2 Cu
$[Cu(mCHNCS_2)]_4$ (B)	I	100-361	126	58.3 (581)	-(2RNC + H_2S)
	II	361-461	417	5.6 (6.0)	-S
	R**			34.4 (35.9)	Cu_2S_2
$[Cu(mTHNCS_2)]_4$ (C)	I	100-300	125	55.3 (54.6)	-(2 RNC + H_2S
	II	300-778	433	12.8 (13.0)	-2S
	R**			31.6 (32.4)	Cu_2S
$[Cu(oAHNCS_2)]_2$ (D)	I	101-423	463	75.0 (75.7)	-(RNCS+H_2S+S)
	R**			23.7 (24.3)	2 Cu
$[Cu(oTHNCS_2)]_2$ (E)	I	101-225	118	46.0 (47.7)	-2 RNC
	II	225-400	262	15.3 (13.4)	-(H_2S+S)
	R**			39.4 (39.0)	Cu_2S_2

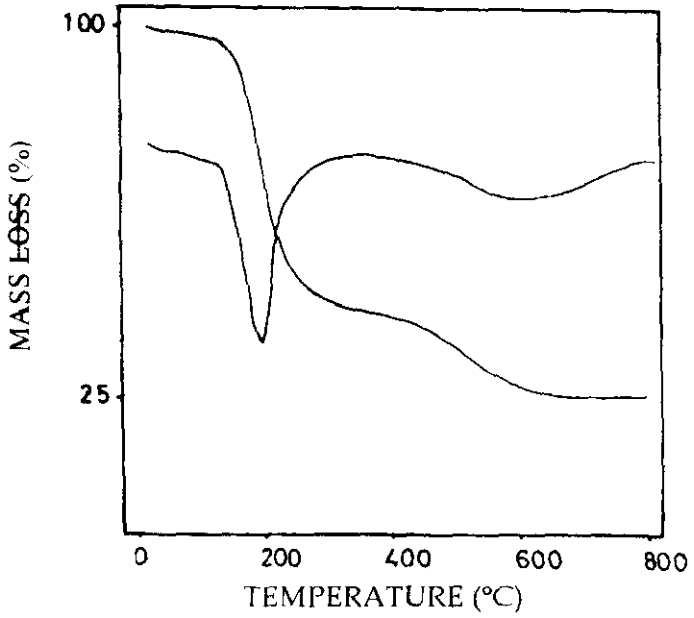

Figure 6.6. TG and DTG curves of $[Cu(PhHNCS_2)]_4$ in nitrogen atmosphere

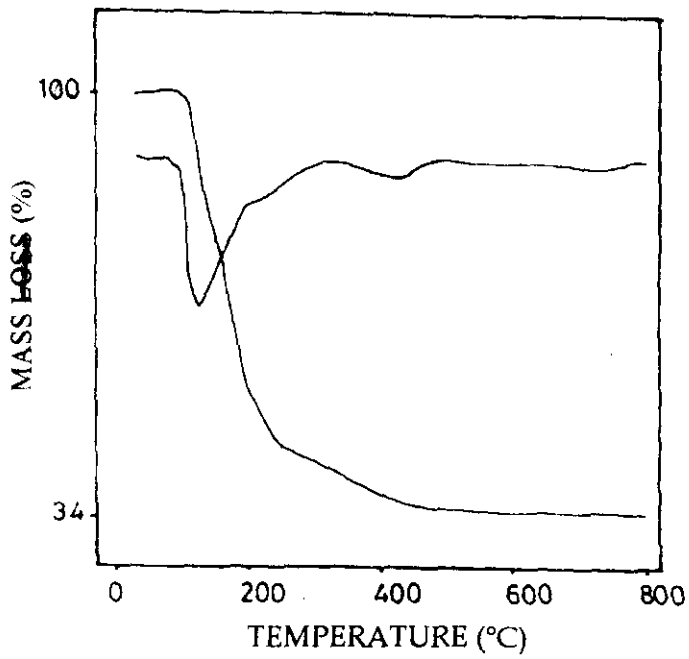

Figure 6.7. TG and DTG curves of $[Cu(mCHNCS_2)]_4$ in nitrogen atmosphere

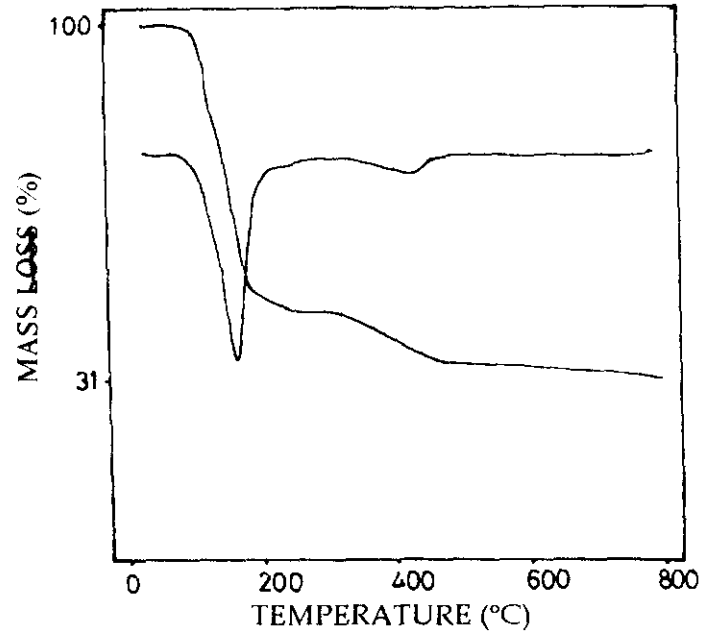

Figure 6.6. TG and DTG curves of $[Cu(mTHNCS_2)]_4$ in nitrogen atmosphere

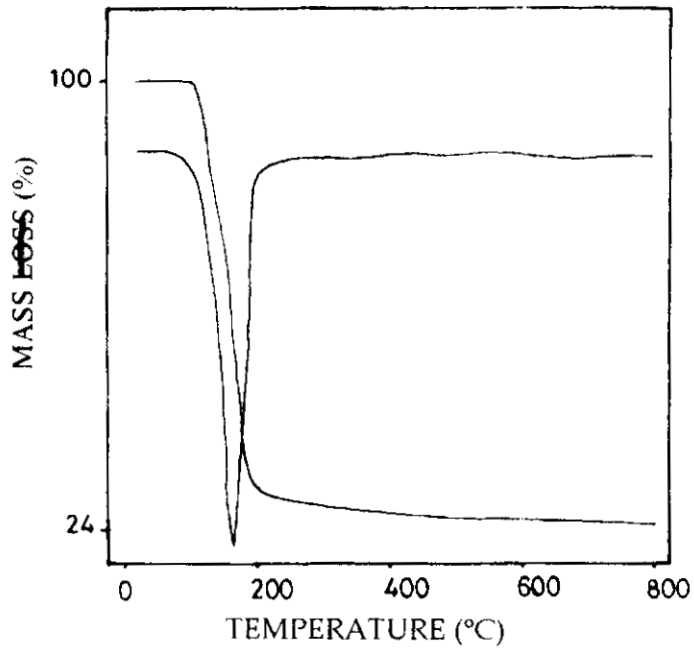

Figure 6.6. TG and DTG curves of $[Cu(oAHNCS_2)]_2$ in nitrogen atmosphere

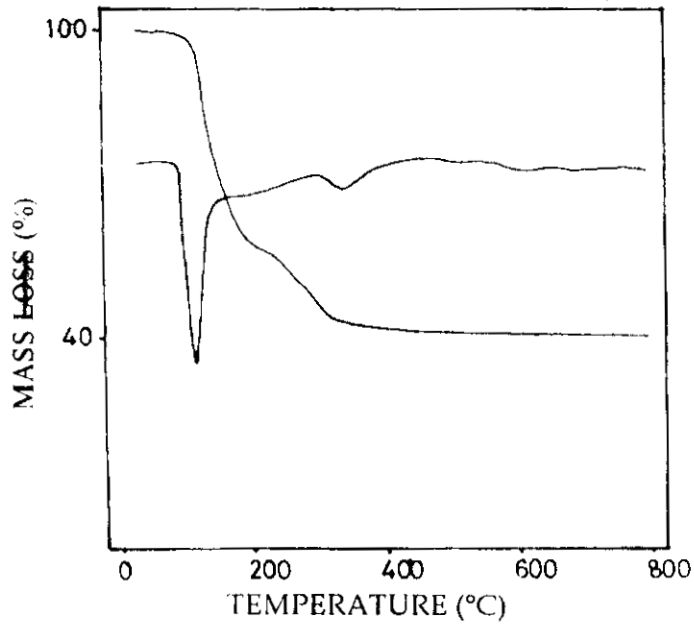

Figure 6.6. TG and DTG curves of $[Cu(oTHNCS_2)]_2$ in nitrogen atmosphere

(ii) Polymers

The thermal decomposition data of the polymeric copper(I) complexes of various monoaryl substituted dithiocarbamates $[Cu(PhHNCS_2)]_n$, $[Cu(MEHNCS_2)]_n$, $[Cu(oCHNCS_2)]_n$, $[Cu(pTHNCS_2)]_n$ and $[Cu(pAHNCS_2)]_n$ are presented in Table 6.5.

Table 6.5. Thermal decomposition data

Compound	Stage	Decomp. temp. range (°C)	DTG_{max} (°C)	Mass loss (%) found (calcd.)	Evolved moiety*
$[Cu(PhHNCS_2)]_n$ (F)	I	138-194	184	51.9 (51.8)	-(2 RNC + H_2S)
	II	260-750	415	6.5 (6.9)	-S
	R**			42.4 (41.3)	Cu_2S_2
$[Cu(mCHNCS_2)]_n$ (G)	I	132-265	186	51.7 (51.7)	-2 RNC
	II	265-638	375	6.7 (6.4)	-H_2S
	R**			41.5 (41.9)	Cu_2S_3
$[Cu(pCHNCS_2)]_n$ (H)	I	138-237	229	56.5 (58.1)	-(2 RNC + H_2S)
	II	237-295	277	6.9 (6.0)	-S
	III	300-700	470	6.3 (6.0)	-S
	R**			30.3 (29.9)	Cu_2S
$[Cu(pTHNCS_2)]_n$ (I)	I	121-284	179	62.1 (61.1)	-(RNC+RNCS+ H_2S)
	II	350-700	460	5.8 (6.5)	-S
	R**			32.1 (32.4)	Cu_2S
$[Cu(pAHNCS_2)]_n$ (J)	I	127-195	180	27.4 (28.7)	-$\frac{1}{2}$ (2 RNC + H_2S)
	II	195-234	221	27.4 (28.7)	-$\frac{1}{2}$ (2 RNC + H_2S)
	III	234-295	226	6.8 (6.1)	-S
	R**			32.88 (30.41)	Cu_2S

The theoretical percentage mass losses and the probable assignment of evolved moieties are also presented in the table. The TG and DTG curves of each stage of decomposition are given in Figures 6.11-6.15. All the complexes start decomposing in the temperature range of 120-140°C. Complexes F, G and I decompose in two stages while H and J decompose in three stages. The final residue per dimeric unit in each case is found to be as (F) Cu_2S_2, (G) Cu_2S_3, (H) Cu_2S, (I) Cu_2S and (J) Cu_2S. The presence of copper and sulphur in all the residues was confirmed by elemental analysis.

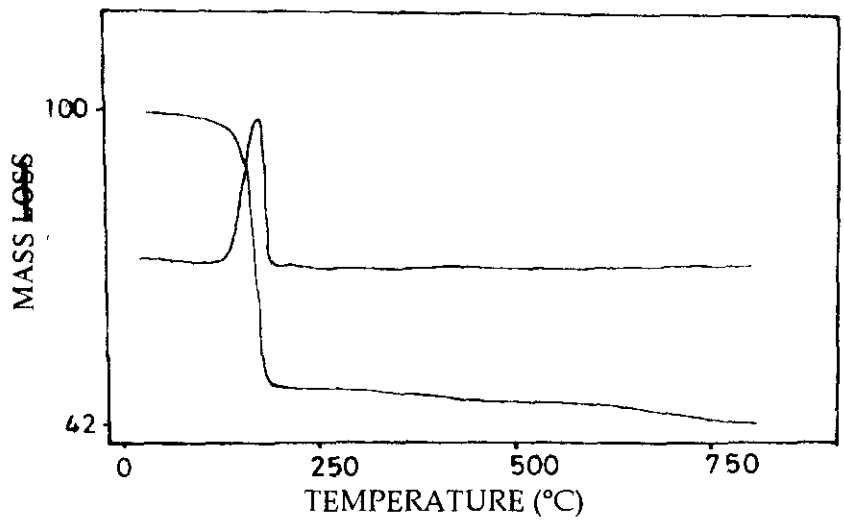

Figure 6.11. TG and DTG curves of $[Cu(pHHNCS_2)]_2$ in nitrogen atmosphere

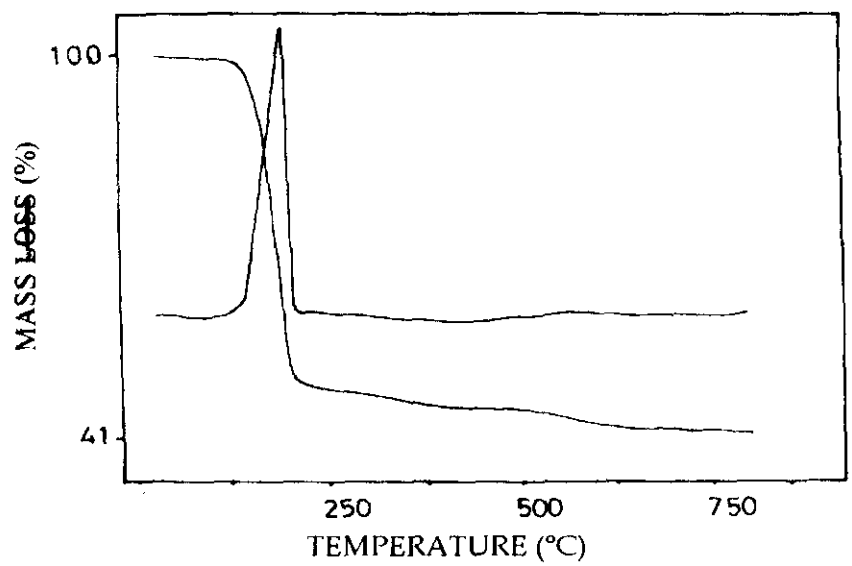

Figure 6.12. TG and DTG curves of $[Cu(mCHNCS_2)]_2$ in nitrogen atmosphere

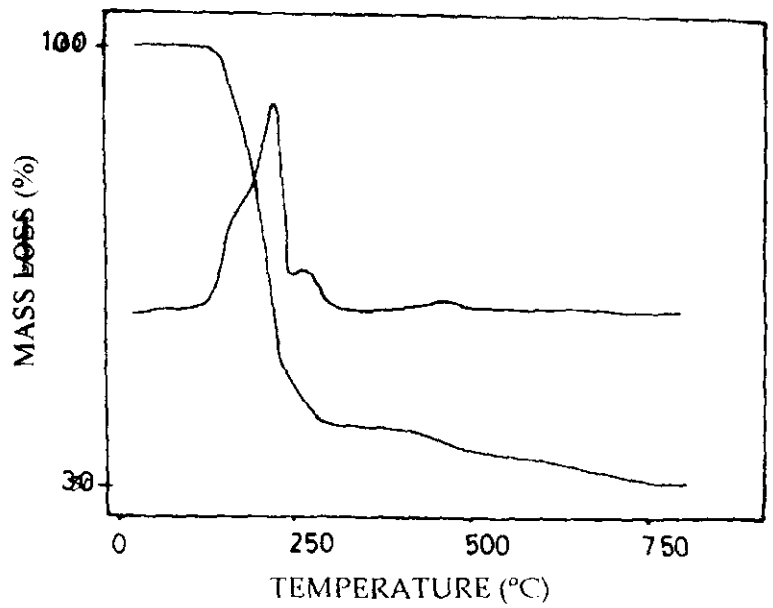

Figure 6.13. TG and DTG curves of $[Cu(pCHNCS_2)]_2$ in nitrogen atmosphere

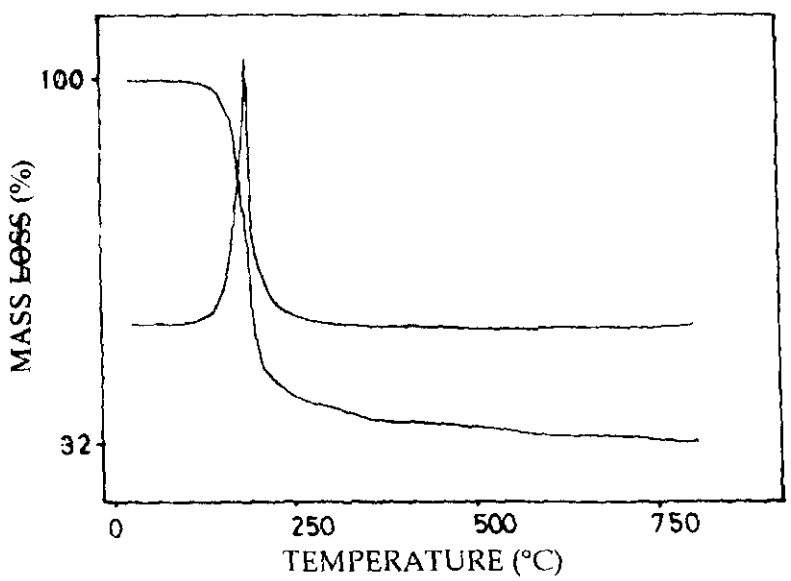

Figure 6.14. TG and DTG curves of $[Cu(pTHNCS_2)]_2$ in nitrogen atmosphere

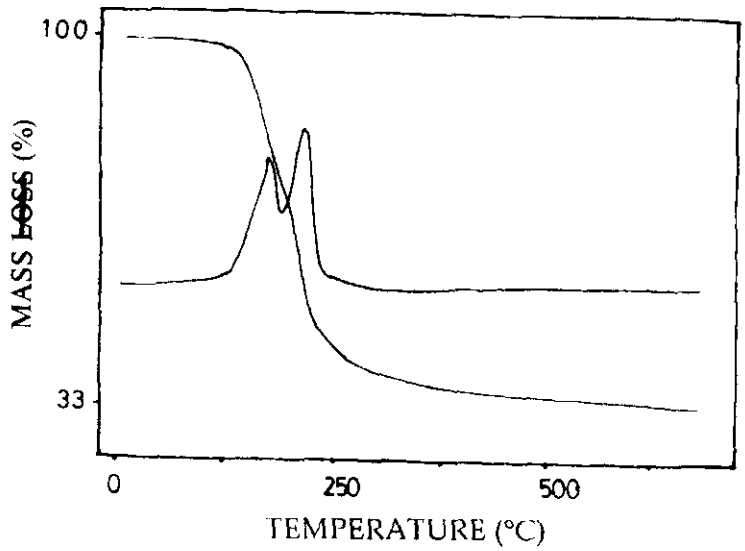

Figure 6.15. TG and DTG curves of [Cu(pAHNCS$_2$)]$_2$ in nitrogen atmosphere

It is quite interesting to note the remarkable variety in the permutation and combination of RNC units, hydrogen and sulphur atoms among the different stages of thermal decomposition depending on the nature of the R group and stereochemisty of the complex. However, from the nature of the decomposition products of the various complexes, it seems that there is a general trend in the mode of thermal decomposition of dimers and polymers. Dimers have a tendency, as seen in the cases of Cu(BuHNCS$_2$)]$_2$ and Cu(oAHNCS$_2$)]$_2$, to form RNCS during decomposition while polymers (including tetramers) in which the sulphur atoms are further coordinated to copper from RNC as shown in Scheme 6.1.

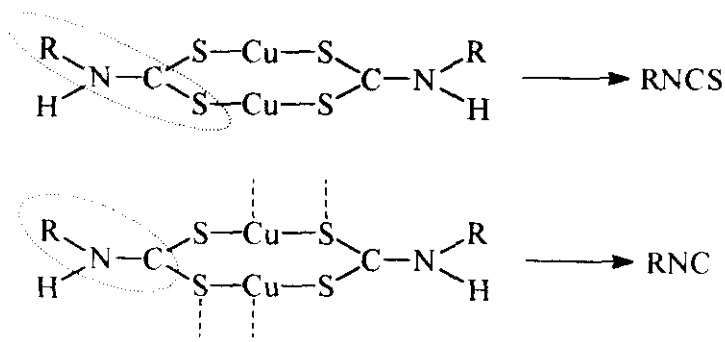

Scheme 6.1

(c) Copper(I) complexes of amino acid derived dithiocarbamates

The mode of thermal decomposition of the two Cu(I) complexes of amino acid derived dithiocarbamates $[Cu(PAHNCS_2)]_2$ and $Cu(CmHNCS_2)]_n$ are found to be quite different from that of the other alkyl/aryl monosubstituted complexes studied so far. This is evident from their thermogram (Figures 6.16 and 6.17) and the phenomenological data of thermal decomposition presented in Table 6.5.

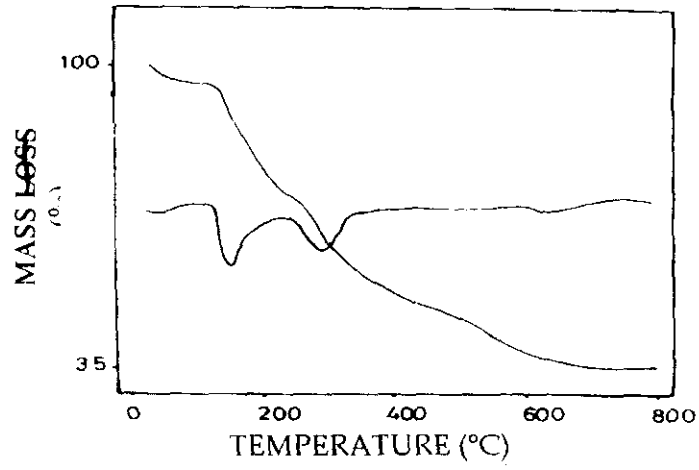

Figure 6.16. TG and DTG curves of $[Cu(PAHNCS_2)]_2$ in nitrogen atmosphere

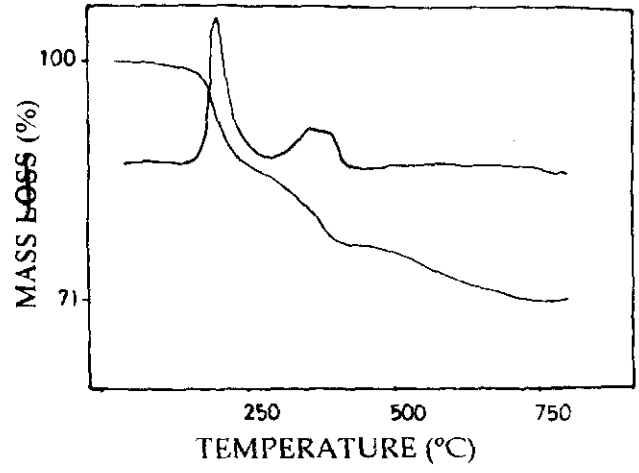

Figure 6.17. TG and DTG curves of $[Cu(CmHNCS_2)]_n$ in nitrogen atmosphere

Table 6.5. Thermal decomposition data

Compound	Stage	Decomp. temp. range (°C)	DTG_{max} (°C)	Mass loss (%) found (calcd.)	Evolved moiety*
$[Cu(PAHNCS_2)]_2$ (A)	I	117-233	153	24.9 (24.4)	-Ph-CH=CH-CO_2H
	II	233-444	292	26.0 (24.4)	-Ph-CH=CH-CO_2H
	III	444-739	631	14.2 (14.5)	-(2 HNC + H_2S)
	R*			34.9 (36.7)	Cu_2S_3
$[Cu(CmHNCS_2)]_n$ (B)	I	154-276	197	13.2 (13.1)	-2 CO
	II	276-425	364	9.2 (8.4)	-H_2O
	III	478-755	520	6.7 (6.6)	-C_2H_4
	R*			71.3 (71.9)	$Cu_2C_2N_2S_4$

Initial decomposition temperatures are 117°C and 154°C for A and B, respectively. Both of them undergo three stage decomposition in nitrogen atmosphere, the final residue being Cu_2S_3 in the case of A and $Cu_2C_2N_2S_4$ (per dimeric unit) of B. Presence of copper and sulphur in the residue of A and copper, nitrogen and sulphur in the residue of B were confirmed by elemental analysis. The mode of thermal decomposition is found to be influenced by the nature of the substituent on α carbon atoms and also due to the presence of the carboxylate moiety. Based on stoichiometric calculation on mass losses during the various decomposition stages, the decomposition for the two complexes can be represented by the following Schemes 6.2a and 6.2b).

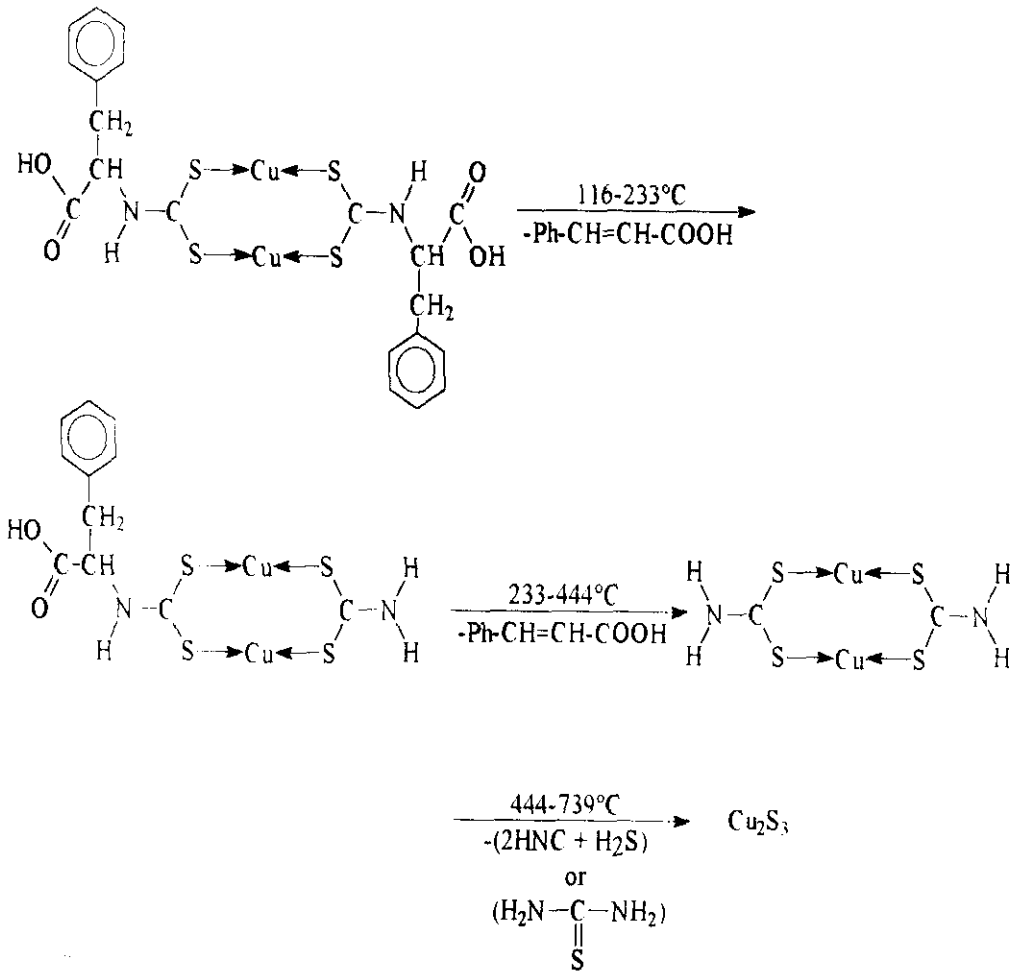
116-233°C
-Ph-CH=CH-COOH
233-444°C
-Ph-CH=CH-COOH
444-739°C
-(2HNC + H2S)
or
(H2N—C—NH2)
S
Cu2S3

Scheme 6.2a

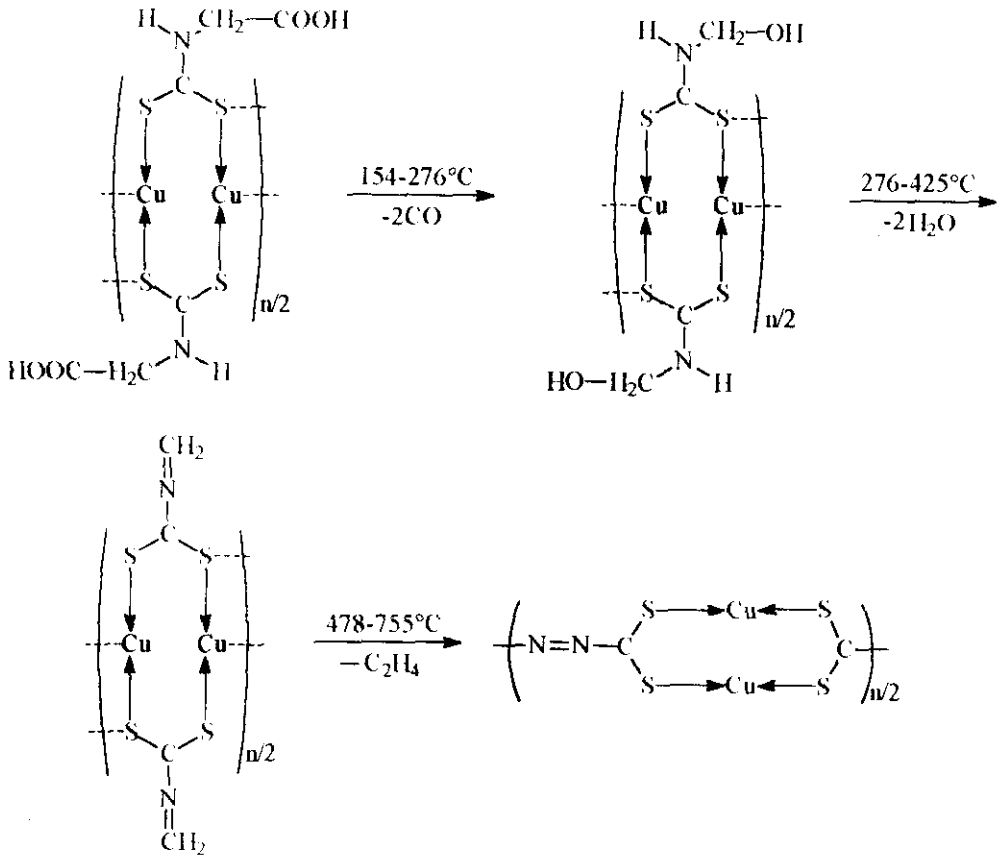

Scheme 6.2b

The decomposition stages I and II are interesting in the case of $[Cu(PAHNCS_2)]_2$ because they involve evolution of a very stable moiety, cinnamic acid. The actual dithiocarbamate-characteristic decomposition is getting initiated only in the Stage III. In the case of $[Cu(CmHNCS_2)]_n$ also the decomposition pattern is seen to be different from other dithiocarbamate complexes as evident from the initial weight losses corresponding to CO, H_2O and C_2H_4.

6.3.2 Thermal stability

Initial decomposition temperature (Ti) and inflection temperature (DTG_{max}) are used to determine the thermal stability of metal chelates.[29] It is evident from the phenomenological data (Tables 6.1-6.5) that the polymeric complexes are thermally more stable than the corresponding oligomeric ones. This may be due to the greater stability the polymers achieved through a

large number of metal-sulphur bridging and metal-metal bonds formed during polymerisation.

(a) N-alkyl dithiocarbamatocopper(I)

The thermal stability of complexes depends primarily on which of the bonds of the complex breaks first at elevated temperatures. If decomposition begins with fission of the bond between the central metal atom and the donor atom, the thermal stability will depend on the strength of this metal-ligand bond.[30] So in these cases the greater stability constant of the complex, greater will be their thermal stability. Decomposition of this type is found to occur with complexes containing volatile ligands (e.g., amine, pyridine and aqueous complexes). On the other hand, the thermal decomposition of chelate complexes proceeds in general, by a different mechanism by breaking some other bond(s) because the chelate ring is seldom split at the coordinate bond. The stability of the complex (i. e. the strength of the coordinate bonds), therefore, influences the thermal stability of the chelate only in so far as it changes the strength of the bond broken first. It has been found that for metal chelates containing the same ligand but different metals, the temperature of decomposition decreases with increase in the stability constant.[31] Thus any enhancement of the strength of the coordinate bond would weaken that bond of the chelate ring which is first ruptured on heating. Venkappayya[23] has suggested that metal chelates of alkyl primary amine-derived dithiocarbamates undergo thermal decomposition by the cleavage of CS bond. Our experimental data suggest that this is true in the case of the present N-alkyldithiocarbamatocopper(I) complexes also. Any factor that decreases the electron flow from N to CS_2 moiety would increase the CS bond order as evident from the canonical form of Dtc as shown in **(2)**.

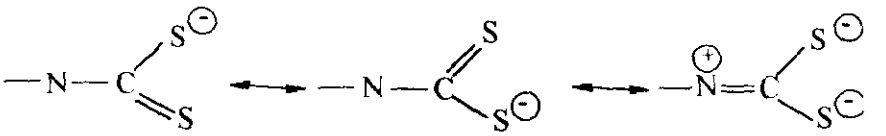

(2)

The fact that the thermal stability of polymeric N-ethyldithiocarbamato-copper(I) is lower than those of N-benzyl and N-butyl derivatives suggests

that cleavage occurs at the CS bond. In the cuprous acetate-type planar linear polymeric structure of $[Cu(RHNC_2)]_n$, due to the steric strain introduced by bulky N-substituents the N-R moiety is slightly tilted out of the plane of CS_2 moiety of Dtc by rotation about CN bond as evidenced by the lower ν(CN) values of the polymeric species compared to those of the corresponding oligomers. Hence, the bulkier the N-substituent the higher the CS bond order and the higher the thermal stability. This explains why the thermal stability of $[Cu(BzHNCS_2)]_n$ or $[Cu(BuHNCS_2)]_n$ with bulkier N-substituent is higher than that of $[Cu(EtHNCS_2)]_n$. This also accounts for the higher thermal stability of polymeric complexes than their corresponding oligomeric species.

(b) N-aryl dithiocarbamatocopper(I) complexes

Among the N-aryldithiocarbamatocopper(I) complexes also, as found in the case of N-alkyl dithiocarbamate complexes, the polymers are thermally more stable than the oligomers. The evolved moieties, during the first stage of thermal decomposition of all the complexes, involve RNC which clearly shows that the decomposition is initiated by the cleavage of CS bond (Tables 6.3 and 6.4). The CN bond order in the polymers is lower than that of the oligomers in N-aryl substituted complexes also (Table 6.5). This reduced CN bond order increases the CS bond order as shown **(2)** increasing the thermal stability of the polymeric complexes. However, it must be noted that even though both the oligomer and polymer has almost the same CN bond order in the case of $Cu(PhHNCS_2)$, the polymer is thermally more stable. This suggests that factors other than the CN bond order contribute to the thermal stability of these complexes.

The modes of decomposition of amino acid derived dithiocarbamate complexes are found to be different from those of the N-alkyl and N-aryl substituted Dtc complexes of copper(I). the decomposition is initiated by the cleavage of C-C or C-N bonds and not C-S bond. Still, the thermal stability of oligomeric $[Cu(PAHNCS_2)]_2$ is comparable to that of other oligomeric $[Cu(RHNCS_2)]$ and thermal stability of $Cu(CmHNCS_2)]_n$ is found to be comparable to that of polymeric $[Cu(RHNCS_2)]_n$. Tables 6.1-6.5.

6.3.3 Kinetic aspects

The kinetic parameters like the activation energy (E) and the pre exponential factor (A) are calculated for well-defined stages of thermal decomposition using Coats and Redfern equations.

$$\log\left[\frac{g(\alpha)}{T^2}\right] = \log\frac{AR}{\phi E}\left[1-\frac{2RT}{E}\right] - \frac{E}{2.303RT}$$

Log $\left[\frac{g(\alpha)}{T^2}\right]$ is plotted against $10^3/T$. From the graphs so obtained (Figures 6.18-6.22) the slope and intercept are determined. From these values the kinetic parameters are calculated using the least square method. The goodness of fit was determined from the correlation coefficient calculated. As mentioned earlier, the relationship, $A = \frac{KT_s}{h} e^{\Delta S/R}$ was used for evaluating the entropy of activation for each stage of thermal decomposition.

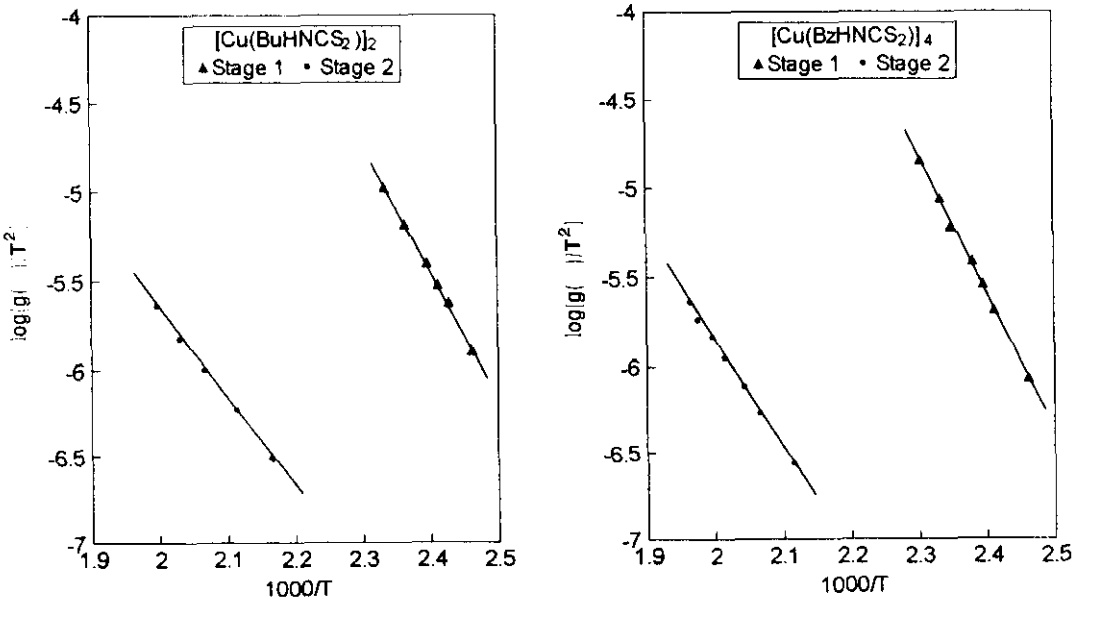

Figure 6.18. log[g(α)/T²] vs. 1000/T plots for the thermal decomposition of oligomeric N-alkyldithiocarbamatocopper(I) complexes

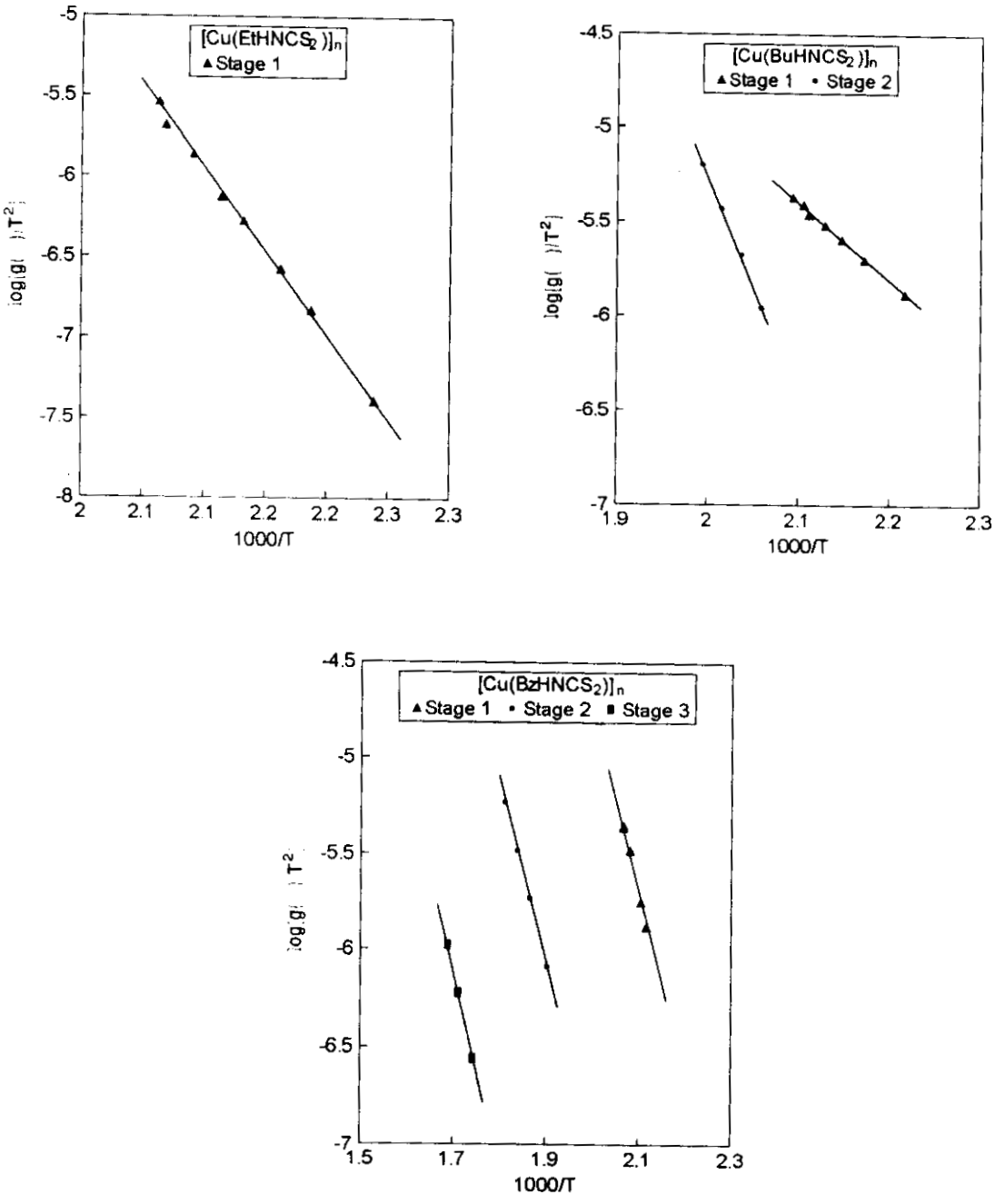

Figure 6.19. log[g(α)/T²] vs. 1000/T plots for the thermal decomposition of polymeric N-alkyldithiocarbamatocopper(I) complexes

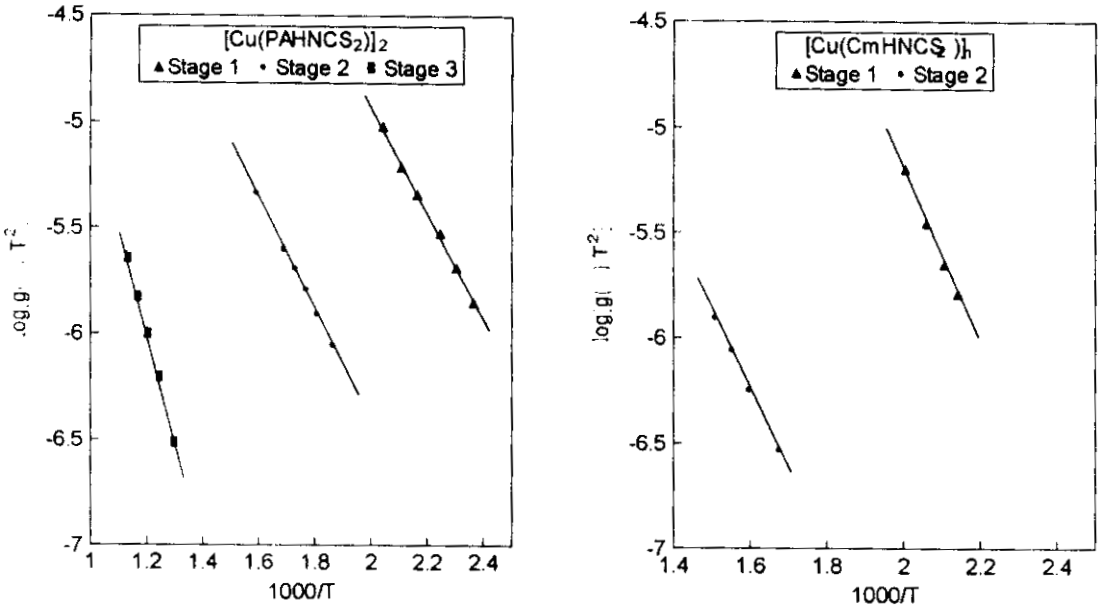

Figure 6.20. ***log[g(α)/T²] vs. 1000/T plots for the thermal decomposition of dithiocarbamates derived from amino acids***

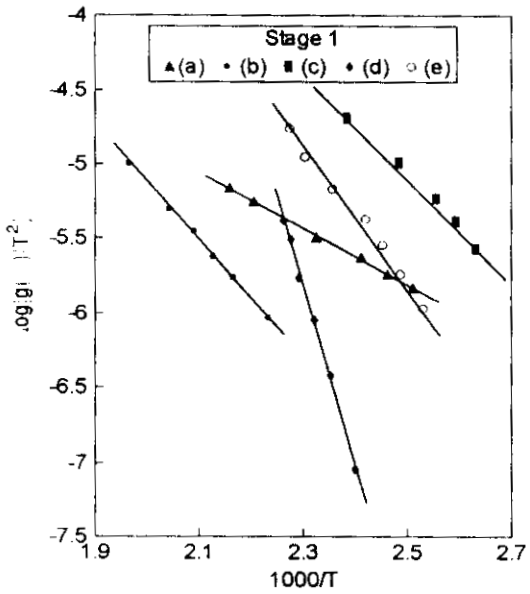

Figure 6.21. ***log[g(α)/T²] vs. 1000/T plots for the thermal decomposition of oligomeric N-aryldithiocarbamatocopper(I) complexes: (a) [Cu(mCHNCS2)]4, (b) [Cu(PhHNCS2)]4, (c) [Cu(oTHNCS2)]2, (d) [Cu(oAHNCS2)]2 and (e) [Cu(mTHNCS2)]4***

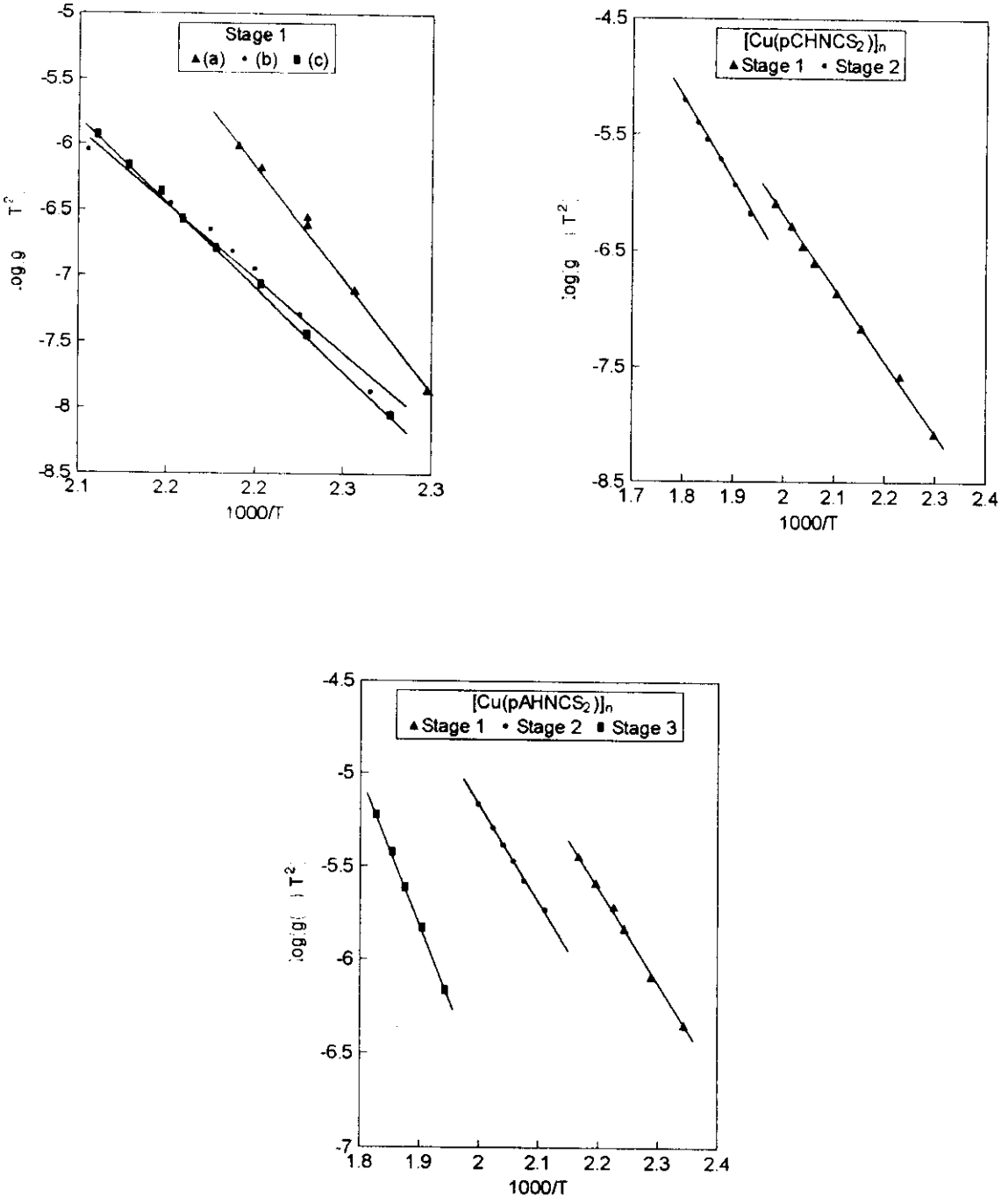

Figure 6.22. ***log[g(α)/T²] vs. 1000/T plots for the thermal decomposition of polymeric N-aryldithiocarbamatocopper(I) complexes: (a) [Cu(PhHNCS₂)]ₙ, (b) [Cu(pTHNCS₂)]ₙ, (c) [Cu(mCHNCS₂)]ₙ, (d) [Cu(pCHNCS₂)]ₙ and (e) [Cu(pAHNCS₂)]ₙ***

(a) N-alkyldithiocarbamatocopper(I) complexes

The kinetic parameters for the thermal decomposition stages of N-alkyldithiocarbamatocopper(I) complexes are presented in Table 6.7.

Table 6.7. Kinetic parameters for the thermal decomposition of N-alkyl dithiocarbamatocopper(I) complexes

Complex	Stage	E(kJ mol^{-1})	A (s^{-1})	ΔS (J mol^{-1})
$[Cu(BuHNCS_2)]_2$ (A)	I	136.61	32.45×10^4	-141.92
	II	97.79	188.57	-205.37
$[Cu(BzHNCS_2)]_4$ (B)	I	147.95	1.26×10^6	-130.80
	II	115.83	1185.23	-190.30
$[Cu(BuHNCS_2)]_n$ (C)	I	254.48	12.81	-48.86
	II	221.93	2.76	-87.88
$Cu(BzHNCS_2]_n$ (D)	I	202.04	5.84	-100.29
	II	178.21	39.90×10^4	-142.77
	III	202.54	59×10^4	-140.14
$[Cu(EtHNCS_2)]_n$ (E)	I	195.46	2.14	-108.82

The activation energies (E) in the different stages of thermal decomposition are in the range 97.79 to 254.48 kJ mol^{-1}. The corresponding values of entropy of activation (ΔS) fall in the range-205.37 to-48.86 J mol^{-1}. The pre-exponential factor vary in the range 2.14 to 32.45×10^4 S^{-1}. There is no definite trend either in the values of E or in the values of ΔS covering the different stages of thermal decomposition of the same complex. The negative values of entropy of activation indicate that the activated complex has a more ordered structure than the reactants and the reactions are slower than normal.[31] But there are definite trends in the values of both E and ΔS for the first stage of decomposition depending on the nature of R group and also on

the stereochemistry of the complex. Activation energy is always found to be higher for the polymer with a less negative value for ΔS than for the corresponding oligomers. This is evident from the values of E and ΔS for complexes A and B and the corresponding polymers C and D (Table 6.8).

Table 6.8. ***Comparison of E and ΔS values for the first stage of thermal decomposition of complexes A and B and their corresponding polymers.***

N-substituent	Benzyl		n-Butyl	
	Oligomer	Polymer	Oligomer	Polymer
E (kJ mol^{-1})	147.95	202.04	136.61	254.48
ΔS (J mol^{-1})	-130.80	-100.29	-141.92	-48.86

The higher activation energy for the first stage decomposition in polymers may be due to the stability achieved by the polymers through a large number of metal-sulphur and metal-metal bonds formed during polymerisation. The higher values of ΔS for the polymers suggest that the transition state for the first stage thermal decomposition of polymers is less ordered than that of the corresponding oligomers.

Trends in the values of E and ΔS for the first stage decomposition of the complexes C, D and E are evident from Table 6.9.

Table 6.9. ***A comparison of E and AS values for the first stage of thermal decomposition of complexes C, D and E***

N-substituent	Ethyl	Benzyl	n-Butyl
E (kJ mol^{-1})	195.46	202.04	254.48
ΔS J mol^{-1})	-108.82	-100.29	-48.86

It is found that the larger the volume occupied by the R group the higher the value of E and the less negative the value of ΔS. This is a clear indication of the cleavage of CS bond rather than MS bond during the first

stage of thermal decomposition as described under the section on thermal stability.

(b) N-aryldithiocarbamatocopper(I) complexes

The kinetic parameters calculated for the thermal decomposition stages of both oligomeric and polymeric N-aryldithiocarbamtocopper(I) are presented in Table 6.10.

Table 6.10. Kinetic parameters for the thermal decomposition of N-aryldithiocarbamatocopper(I) complexes

Complex	Stage	E (kJ mol^{-1})	A (s^{-1})	ΔS (J mol^{-1})
$[Cu(Ph\ HNS_2)]_4$ (A)	I	73.60	19.10	-224.02
$[Cu(mCHNCS_2)]_4$ (B)	I	35.93	0.24	-259.30
$[Cu(mTHNCS_2)]_4$ (C)	I	85.98	395.42	-198.25
$[Cu(oTHNCS_2)]_2$ (D)	I	66.92	52.65	-214.21
$[Cu(oAHNCS_2)]_2$ (E)	I	229.67	1.32×10^{10}	-54.33
$[Cu(PhHNCS_2)]_n$ (F)	I	350.72	20.23	52.47
$[Cu(mCHNCS_2)]_n$ (G)	I	243.06	5.74	-61.81
$[Cu(pTHNCS_2)]_n$ (H)	I	133.95	4.79×10^4	-158.77
$[Cu(pCHNCS_2)]_n$ (I)	I	118.45	11.33×10^2	-190.76
	II	141.72	97.32×10^2	-173.64
$[Cu(pA\ NCS_2)]_n$ (J)	I	99.46	672.70	-194.255
	II	98.41	324.29	-201.04
	III	154.82	4.37×10^4	-160.99

The activation energies in the first stage of thermal decomposition of the oligomeric complexes are in the range 35.93–229.67 kJ mol^{-1}. The corresponding values of the entropy of activation fall in the range -259.30 – -54.33 J mol^{-1}. The values of pre-exponential factor (A) vary from 1.32×10^{10} – 19.1 s^{-1}. It is observed that systems requiring higher entropy of activation need only less energy of activation for the thermal decomposition. Only $[Cu(oAHNCS_2)]_2$ is found to have a comparatively high value of activation energy. As indicated by IR data [ν(CN): 1495] the phenyl ring remains out of the plane of the NCS_2 moiety because of the presence of $-OCH_3$ substituent at the orthoposition. This orientation of the phenyl ring influences the decomposition mechanism in some way, increasing the activation energy. In fact, this is the only oligomeric complex which is not found to decompose in the first stage according to Mampel model (Section **6.3.4**).

The values of activation energies in the different stages of thermal decomposition of the polymeric complexes are in the range 98.41 to 350 kJ mol^{-1}. The corresponding values of entropy of activation fall in the range 201.04 to 52.47 J mol^{-1}. As found in the case of oligomeric complexes, systems requiring lower entropy of activation, whether positive or negative, need higher energy of activation for its thermal decomposition. The higher values of the energy of activation in the first stage of thermal decomposition of the polymeric complexes compared to those of the oligomeric complexes may be due to the greater stability the polymers attained through a large number of metal-sulphur and metal-metal bond formation during polymerisation. There is no definite trend in the values of E or ΔS among the different stages of decomposition of the same complex. Polymeric $[Cu(PhHNCS_2)]_n$ is the only complex with positive entropy of activation for its first stage of thermal decomposition. This indicates that its activated complex has a less ordered structure than the reactant.[31]

The kinetic parameters for the different stages of thermal decomposition of the Cu(I) complexes $[Cu(PAHNCS_2)]_2$ and $[Cu(CmHNCS_2)]$ are given in Table 6.11.

Table 6.11. Kinetic parameters for the thermal decomposition of Cu(I) complexes of aminoacid-derived dithiocarbamates

Complex	Stage	E (kJ mol^{-1})	A (s^{-1})	ΔS (J mol^{-1})
$[Cu(PAHNCS_2)]$	I	48.20	1.08	-247.21
	II	50.36	0.32	-259.68
	III	99.63	2.58	-246.52
$[Cu(CmHNCS_2]_n$	I	77.23	26.65	-221.39
	II	72.16	1.16	-250.02

The activation energies E, for the first two stages of thermal decomposition of $[Cu(PAHNCS_2)]_2$ which involves the elimination of two cinnamic acid molecules successively, are found to be almost the same, 48.2 and 50.36 kJ mol^{-1} respectively. The corresponding values of entropy of activation (ΔS) are-247.21 and-259.68 J mol^{-1}, the pre exponential factors being 1.08 and 0.32 S^{-1} respectively. In the case of $[Cu(CmHNCS_2)]_n$ the first two stages which involve the elimination of carbon monoxide and water respectively are found to have the activation energies of 77.23 and 72.16 kJ mol^{-1}, the corresponding values of entropy of activation ΔS being -221.39 and -250.02 J mol^{-1} and the pre-exponential factors being 26.65 and 1.16 s^{-1}, respectively. The negative values of the entropy of activation indicate that the activated complex has a more ordered structure than the reactant. The very, low values of activation energies (E) for the various stages suggest that the Dtc moiety may be strongly bound to the metal in the chelate thereby weakening the other bonds which undergo cleavage. This is also indicated by the composition of the residues, which are found to retain most of the sulphur atoms coordinated to the metal.

6.3.4 Mechanistic aspects

The elucidation of mechanisms of solid state thermal decomposition reaction is a complicated one. Several kinetic equations have been derived corresponding to the three possible types of rate determining steps during thermal decomposition, viz., nucleation and growth, diffusion and phase boundary reactions. The kinetic equations which govern the reaction mechanism are based on the assumption that the form of g(α) depends on the reactions mechanism. Out of the nine forms of g(α) proposed by Satava,[32] the form of g(α) which gives the best representation of the experimental data is considered as the mechanism of the reaction. The correlation coefficients obtained for the nine forms of g(α) for the various stages of thermal decomposition of the complexes are presented in Tables 6.12-6.16.

Table 6.12. Correlation coefficients calculated using the nine forms of g(α) for oligomeric N-alkyl dithiocarbamatocopper(I) complexes

No.	Form of g(α)	Correlation coefficient (γ)			
		$[Cu(BuHNCS_2)]_2$		$[Cu(BzHNCS_2)]_4$	
		Stage I	Stage II	Stage I	Stage II
1	$-\ln(1-\alpha)$	-0.9995	-0.9974	-0.9990	-0.9974
2	$1-(1-\alpha)^{1/2}$	-0.9947	-0.9987	-0.9934	-0.9993
3	$1-(1-\alpha)^{1/3}$	-0.9968	-0.9993	-0.9964	-0.9989
4	$\alpha+(1-\alpha)\ln(1-\alpha)$	-0.9920	-0.9970	-0.9892	-0.9989
5	$[1-(2\alpha/3)-(1-\alpha)^{2/3}$	-0.9940	-0.9984	-0.9923	-0.9992
6	$[-\ln(1-\alpha)]^{1/2}$	-0.9993	-0.9970	-0.9989	-0.9971
7	$[-\ln(1-\alpha)]^{1/3}$	-0.9993	-0.9966	-0.9989	-0.9966
8	$[1-(1-\alpha)^{1/3}]^2$	-0.9828	-0.9920	-0.9769	-0.9666
9	α^2	-0.9855	-0.9899	-0.9802	-0.9971

Table 6.13. Correlation coefficients calculated using the nine forms of g(α) for polymeric N-alkyl dithiocarbamatocopper(I) complexes

No.	Form of g(α)	Correlation coefficient (γ)					
		$[Cu(BuHNCS_2)]_n$		$[Cu(BzHNCS_2)]_n$			$[Cu(EtHNCS_2)]_n$
		Stage I	Stage II	Stage I	Stage II	Stage III	Stage I
1	-ln(1-α)	-0.9702	-0.9996	-0.9992	-0.9999	-0.9995	-0.9913
2	1-(1-α)1/2	-0.9921	-0.9963	-0.9813	-0.9977	-0.9998	-0.9982
3	1-(1-α)1/3	-0.9865	-0.9977	-0.9898	-0.9992	-0.9999	-0.9966
4	α+(1-α)ln(1-α)	-0.9969	-0.9947	-0.9687	-0.9964	-0.9994	-0.9990
5	[1-(2α/3)-(1-α)2/3	-0.9943	-0.9966	-0.9777	-0.9977	-0.9996	-0.9987
6	[-ln(1-α)]1/2	-0.9679	-0.9994	-0.9988	-0.9999	-0.9997	-0.9902
7	[-ln(1-α)]1/3	-0.9650	-0.9993	-0.9986	-0.9998	-0.9991	-0.9888
8	[1-(1-α)1/3]2	-0.9990	-0.9897	-0.9389	-0.9912	-0.9978	-0.9976
9	α2	-0.9992	-0.9907	-0.9474	-0.9924	-0.9980	-0.9981

Table 6.14. Correlation coefficients calculated using the nine forms of g(α) for oligomeric N-aryl dithiocarbamatocopper(I) complexes

No.	Form of g(α)	Correlation coefficient (γ)				
		$[Cu(PhHNCS_2)]_4$	$[Cu(mCHNCS_2)]_4$	$[Cu(mTHNCS_2)]_4$	$[Cu(oTHNCS_2)]_2$	$[Cu(oAHNCS_2)]_4$
		Stage I	Stage I	Stage I	Stage I	Stage I
1	-ln(1-α)	-0.9994	-0.9993	-0.9959	-0.9958	-0.9894
2	1-(1-α)1/2	-0.9920	-0.9985	-0.9850	-0.9743	-0.9979
3	1-(1-α)1/3	-0.9958	-0.9990	-0.9908	-0.9839	-0.9963
4	α+(1-α)ln(1-α)	-0.9876	-0.9981	-0.9803	-0.9643	-0.9984
5	[1-(2α/3)-(1-α)2/3	-0.9914	-0.9987	-0.9851	-0.9739	-0.9983
6	[-ln(1-α)]1/2	-0.9993	-0.9990	-0.9951	-0.9946	-0.9884
7	[-ln(1-α)]1/3	-0.9990	-0.9975	-0.9942	-0.9930	-0.9875
8	[1-(1-α)1/3]2	-0.9664	-0.9920	-0.9572	-0.9120	-0.9952
9	α2	-0.9769	-0.9961	-0.9675	-0.9429	-0.9959

Table 6.15. Correlation coefficients calculated using the nine forms of g(α) for polymeric N-aryl dithiocarbamatocopper(I) complexes

No.	Form of g(α)	Correlation coefficient (γ)							
		$[Cu(PhHNCS_2)]_n$	$[Cu(mCHNCS_2)]_n$	$[Cu(pTHNCS_2)]_n$	$[Cu(pCHNCS_2)]_n$		$[Cu(pAHNCS_2)]_n$		
		Stage I	Stage I	Stage I	Stage I	Stage II	Stage I	Stage II	Stage III
1	-ln(1-α)	-0.9826	-0.9902	-0.9993	-0.9920	-0.9990	-0.9951	-0.9989	-0.9993
2	1-(1-α)1/2	-0.9988	-0.9996	-0.9895	-0.9987	-0.9955	-0.9990	-0.9955	-0.9959
3	1-(1-α)1/3	-0.9960	-0.9983	-0.9941	-0.9974	-0.9972	-0.9989	-0.9977	-0.9975
4	α+(1-α)ln(1-α)	-0.9984	-0.9989	-0.9837	-0.9990	-0.9932	-0.9977	-0.9913	-0.9937
5	[1-(2α/3)-(1-α)2/3	-0.9991	-0.9996	-0.9881	-0.9990	-0.9950	-0.9988	-0.9942	-0.9954
6	[-ln(1-α)]1/2	-0.9815	-0.9892	-0.9990	-0.9902	-0.9989	-0.9945	-0.9991	-0.9992
7	[-ln(1-α)]1/3	-0.9802	-0.9881	-0.9987	-0.9876	-0.9989	-0.9939	-0.9989	-0.9993
8	[1-(1-α)1/3]2	-0.9924	-0.9939	-0.9659	-0.9956	-0.9854	-0.9919	-0.9909	-0.9870
9	α2	-0.9934	-0.9948	-0.9717	-0.9971	-0.9878	-0.9935	-0.9831	-0.9888

Table 6.16. Correlation coefficients calculated using the nine forms of g(α) for copper(I) complexes of dithiocarbamates derived from amino acids

No.	Form of g(α)	Correlation coefficient (γ)				
		$[Cu(pAHNCS_2)]_2$			$[Cu(CmHNCS_2)]_n$	
		Stage I	Stage II	Stage III	Stage I	Stage II
1	$-\ln(1-\alpha)$	-0.9991	-0.9996	-0.9991	-0.9999	-0.9983
2	$1-(1-\alpha)^{1/2}$	-0.9949	-0.9955	-0.9994	-0.9980	-0.9997
3	$1-(1-\alpha)^{1/3}$	-0.9972	-0.9977	-0.9967	-0.9989	-0.9997
4	$\alpha+(1-\alpha)\ln(1-\alpha)$	-0.9927	-0.9938	-0.9926	-0.9969	-0.9995
5	$[1-(2\alpha/3)-(1-\alpha)^{2/3}$	-0.9950	-0.9958	-0.9945	-0.9980	-0.9997
6	$[-\ln(1-\alpha)]^{1/2}$	-0.9988	-0.9995	-0.9987	-0.9967	-0.9980
7	$[-\ln(1-\alpha)]^{1/3}$	-0.9986	-0.9973	-0.9976	-0.9990	-0.9973
8	$[1-(1-\alpha)^{1/3}]^2$	-0.9744	-0.9746	-0.9797	-0.9938	-0.9979
9	α^2	-0.9856	-0.9874	-0.9869	-0.9938	-0.9979

From the tables it is evident that, though the reaction mechanisms for the second and further stages of thermal decomposition are not directly influenced by the original geometry and stereochemistry of the complexes, these factors influence the mechanism of the first stage of thermal decomposition of the various complexes. The form of g(α) with the highest values of correlation coefficient for the first stage of thermal decomposition of the complexes are given in Table 6.17.

Table 6.17. The forms of g(α) with the highest value of correlation coefficient and the corresponding rate controlling process.

Complex	Form of g(α)	Rate controlling process for the first stage of thermal decomposition
$[Cu(BuHNCS_2)]_2$	-ln (1-α)	Random nucleation, one nucleus on each particle, Mampel equation
$[Cu(BzHNCS_2)]_4$	"	"
$[Cu(PAHNCS_2)]_2$	"	"
$[Cu(PhHNCS_2)]_4$	"	"
$[Cu(mCHNCS_2)]_4$	"	"
$[Cu(mTHNCS_2)]_4$	"	"
$[Cu(oTHNCS_2)]_2$	"	"
$[Cu(oAHNCS_2)]_2$	(1-α) ln (1-α) + α	Two dimensional diffusion cylindrical symmetry
$[Cu(BuHNCS_2)]_n$	α^2	One dimensional diffusion
$[Cu(EtHNCS_2)]_n$	(1-α) ln (1-α) + α	Two dimensional diffusion cylindrical symmetry
$[Cu(BzHNCS_2)]_n$	-ln (1-α)	random nucleation, one nucleus on each particle; Mampel equation
$[Cu(CmHNCS_2)]_n$	"	"
$[Cu(pTHNCS_2)]_n$	"	"
$[Cu(PhHNCS_2)]_n$	$\left(1-\frac{2}{3}\alpha\right)-(1-\alpha)^{2/3}$	Three dimensional diffusion, spherical symmetry; Ginstling-Brownshtein equation
$[Cu(m\ CHNCS_2)]_n$	"	"
$[Cu(pCHNCS_2)]_n$	"	"
$[Cu(pAHNCS_2)]_n$	$1-(1-\alpha)^{2/3}$	Phase boundary reaction, cylindrical symmetry

For the first stage of thermal decomposition of all the oligomeric complexes except $[Cu(oAHNCS_2)]_2$ whether N-alkyl substituted, N-aryl substituted or N-carboxy alkyl substituted, the highest values of the magnitude of correlation coefficient are obtained for the equation $g(\alpha) = -\ln(1-\alpha)$. Hence the mechanism is random nucleation with one nucleus on each particle representing 'Mampel model'. The planarity of these oligomeric complexes may be responsible for this reaction mechanism. In $[Cu(oAHNCS_2)]_2$, the phenyl ring is not in the plane of NCS_2 moiety as indicated by IR data mentioned earlier, and it decomposes by two dimensional diffusion, cylindrical symmetry. It is also worthwhile to note that for the first stage of thermal decomposition of most of the polymeric complexes, the rate controlling process is not represented by 'Mampel model'. For $[(BuHNCS_2)]_n$ and $[Cu(EtHNCS_2)]_n$ the highest values of correlation coefficient are obtained for equation with $g(\alpha) = \alpha^2$ and $g(\alpha) = (1-\alpha)\ln(1-\alpha) + \alpha$ corresponding to the rate determining process of one dimensional diffusion of spherical symmetry and two dimensional diffusion of cylindrical symmetry, respectively. In the first stage of thermal decomposition of $[Cu(PhHNCS_2)]_n$, $[Cu(mCHNCS_2)]_n$ and $[Cu(pCHNCS_2)]_n$ the rate controlling process are represented by 'Ginstling-Brownstein' equation of three dimensional diffusion, spherical symmetry. In the case of $[Cu(PAHNCS_2)]_n$ the rate controlling process is phase boundary reaction of cylindrical symmetry, represented by the equation with $g(\alpha) = 1-(1-\alpha)^{1/2}$. Only in the case of the three polymeric complexes $[Cu(BzHNCS_2)]_n$, $[Cu(pTHNCS_2)]_n$ and $[Cu(CmHNCS_2]_n$, the rate controlling process of the first stage of thermal decomposition is represented by 'Mampel model'.

References

1. M. Delepine, *Compt. Rend.*, **146**, 981 (1908).
2. M. Delepine, *Bull., Soc. Chem.Fr.*, **3**, 643 (1908).
3. G. D'. Ascenzo and W. W. Wendlandt, *J. Therm. Anal.*, **1**, 423 (1969).
4. C. G. Sceney and R. J. Magee, *J. Inorg. Nucl. Chem. Lett.*, **9**, 595 (1973).
5. A. Tavlaridis and R. Neeb, *Z. Anal. Chem.*, **282**, 17 (1976).
6. J. Krupchik, J. Garaj, S. Holotik, D. Oktavec and M. Kosik, *J. Chromatogr.*, **112**, 189 (1975).
7. J. Masaryk, J. Krupchik, J. Garaj and M. Kosik, *J. Chromatogr.*, **115**, 256 (1978).
8. D. C. Hilderbrand and E. E. Pickett, *Anal. Chem.*, **47**, 425 (1975).
9. A. K. Sharma, *Thermochim. Acta*, **104**, 339 (1986).
10. S. V. Larionov, L. A. Kosareva, A. F. Malikova and A. A. Shklyaev, *Zhur. Neorg. Khim.*, **22**, 2401 (1977).
11. S. Kumar and N. K. Kaushik, *Indian J. Chem.*, **20A**, 512 (1981).
12. N. K. Kaushik, G. R. Chhatwal and A. K. Sharma, *J. Thermal Anal.*, **26**, 309 (1983).
13. N. K. Kaushik, B. Bhushan and A. K. Sharma, *Thermochim. Acta*, **76**, 345 (1984).
14. N. K. Kaushik, B. Bhushan and A. K. Sharma, *Transition Met. Chem.*, **9**, 250 (1984).
15. N. K. Kaushik, B. Bhushan and A. K. Sharma, *Thermal Analysis Proc. 8th ICTA, Thermochim. Acta*, **93**, 105 (1985).
16. B. Bhushan, A. K. Sharma and N. K. Kaushik, *Bull. Soc. Chim. Fr.*, 1293 (1983).
17. B. Macias, J. J. Criado, M. V. Vaquero and M. V. Villa, *Thermochim. Acta*, **223**, 213 (1993).
18. H. B. Singh, S. Maheswari and H. Tomer, *Thermochim. Acta*, **64**, 47 (1983).
19. J. J. Criado and B. Macias, *Thermochim. Acta*, **127**, 101 (1988).
20. H. B. Singh, S. Maheswari, S. Srivastava and V. Rani, *Synth. React. Met.-Org. Chem.*, **12**, 659 (1982).
21. G. A. Katsoulos, M. L. Kantouri, C. C. Hadjikostar and P. Kokorotsikos, *Thermochim. Acta*, **149**, 331 (1989).
22. M. A. Bernard and M. M. Borel, *Bull. Soc. Chim. Fr.*, 3066 (1969).
23. D. Vaenkappyya and D. H. Brown, *Indian J. Chem.*, **12**, 838 (1974).
24. S. Kumar, N. K. Kaushik, I. P. Mittal, *Thermal Analysis Proc. VI Int. Conf.*, Bayreuth, 1980.
25. G. K. Bratspies, J. F. Smith and J. O. Hill, *Thermochim. Acta*, **19**, 373 (1977).

26. N. K. Kaushik, G. R. Chhatwai and A. K. Sharma, *Thermochim. Acta,* **58**, 231 (1982).

27. J. Sestak and G. Berggren, *Thermochim. Acta,* **3**, 1 (1971).

28. A. W. Coats and J. P. Redfern, *Nature (London),* **201**, 68 (1964).

29. V. Seshagiri and S. Rao, *Fresenius, Z. Anal. Chem.,* **39**, 1024 (1967).

30. K. Burger, *Coordination Chemistry: Experimental Methods,* London, Butterworth, 1973.

31. S. Mathew, C. G. R. Nair and K. Muraleedharan, *Thermochim. Acta,* **155**, 247 (1989).

32. V. Satava, *Thermochim. Acta,* **2**, 423 (1971).